J. Mol. Biol. (1996) **264**, 919–932

JMB

Scanning Force Microscopy of DNA Deposited onto Mica: Equilibration *versus* Kinetic Trapping Studied by Statistical Polymer Chain Analysis

Claudio Rivetti[1], Martin Guthold[1,2] and Carlos Bustamante[1,3,4]*

[1]*Institute of Molecular Biology, University of Oregon, Eugene, OR 97403 USA*

[2]*Physics Department University of Oregon Eugene, OR 97403, USA*

[3]*Chemistry Department University of Oregon Eugene, OR 97403, USA*

[4]*Howard Hughes Medical Institute, University of Oregon, Eugene, OR 97403 USA*

**Corresponding author*

This paper reports a study of the deposition process of DNA molecules onto a mica surface for imaging under the scanning force microscope (SFM). Kinetic experiments indicate that the transport of DNA molecules from the solution drop onto the surface is governed solely by diffusion, and that the molecules are irreversibly adsorbed onto the substrate. A statistical polymer chain analysis has been applied to DNA molecules to determine the deposition conditions that lead to equilibrium and those that result in trapped configurations. Using the appropriate conditions, DNA molecules deposited onto freshly cleaved mica, are able to equilibrate on the surface as in an ideal two-dimensional solution. A persistence length of 53 nm was determined from those molecules. DNA fragments that were labeled on both ends with a horseradish peroxidase streptavidin fusion protein were still able to equilibrate on the surface, despite the additional protein-surface interaction. In contrast, DNA molecules deposited onto glow-discharged mica or H^+-exchanged mica do not equilibrate on the surface. These molecules adopt conformations similar to those expected for a simple projection onto the surface plane, suggesting a process of kinetic trapping.

These results validate recent SFM application to quantitatively analyze the conformation of complex macromolecular assemblies deposited on mica. Under equilibration conditions, the present study indicates that the SFM can be used to determine the persistence length of DNA molecules to a high degree of precision.

Keywords: scanning force microscopy; DNA deposition; DNA persistence length; excluded volume effects; mica

Introduction

The scanning force microscope (SFM) known also as the atomic force microscope (Binnig *et al*., 1986) is becoming a widely used tool to investigate the structure of proteins, DNA and protein-DNA complexes at a nanometer scale (Rees *et al*., 1993; Bustamante *et al*., 1994a; Wyman *et al*., 1995). This microscope generates an image by probing the surface of the sample with a sharp tip attached to the end of a flexible cantilever. Small forces of interaction between the sample and the tip produce a deflection of the cantilever that is detected and converted into height information. By plotting the heights for each position of the tip over the sample, the topography of the sample can be reconstructed (Bustamante *et al*., 1993; Hansma & Hoh, 1994).

Based on this principle, biological molecules deposited onto an ultra-flat surface can be imaged without the use of contrast enhancement techniques (Lyubchenko *et al*., 1993). One of the most attractive features of the SFM is that it can operate equally well with the cantilever immersed in liquid as in air, making it possible to image biological molecules under physiological conditions. Several substrates have been used and many deposition protocols now exist to reproducibly attach biological samples to the substrate (Lyubchenko *et al*., 1991; Lindsay *et al*., 1992; Thundat *et al*., 1992;

Present address: Claudio Rivetti, Instituto di Scienze Biochimiche, Università di Parma, viale delle Scienze, 43100 Parma, Italy.

Abbreviations used: SFM, scanning force microscopy; EM, electron microscopy; 2D, two dimensions; 3D, three dimensions.

0022–2836/96/500919–14 $25.00/0

Schaper *et al*., 1993; Rabke *et al*., 1994) but the process by which the molecules approach the surface and bind to it remains unclear.

During deposition, the conformation of long polymers, such as DNA, is inevitably modified by the transition from three to two dimensions (Lang *et al*., 1967). The loss of one degree of freedom drastically reduces the number of possible configurations that the molecules can access within the range of the thermal energy. In principle, two extreme cases of molecule-surface interactions can be described: (1) the molecules freely equilibrate on the surface as in a 2D solution before they are captured in a particular conformation; or (2) the molecules adhere without having equilibrated on the substrate, and the resulting conformation resembles a projection of the actual 3D conformation onto the surface. Since the polymer contour length must be conserved during the 3D to 2D transition, the shape of the molecules on the surface will deviate somewhat from a true mathematical projection.

For a deposition process as described in (1), the molecules on the surface represent an ensemble of the lowest energy conformations of molecules existing in a two-dimensional space, thus, meaningful information about the structure of the molecules can be extracted from the 2D images. In case (2), the conformations of the molecules reflect the history of their approach to the surface and it is therefore difficult to distinguish between intrinsic conformations of the molecule and those induced by the surface adsorption. The latter scenario corresponds to kinetic trapping of the molecules onto the surface.

Consequently, a quantitative interpretation of two-dimensional images of DNA and protein-DNA complexes requires an understanding of whether and how the adsorption process, and the resulting change in dimensions, affect the conformation of the molecules. DNA persistence length studies and measurements of intrinsic or protein-induced DNA bend angles by high-resolution microscopies (Frontali *et al*., 1979; Rees *et al*., 1993; Erie *et al*., 1994; Hansma *et al*., 1994; Griffith *et al*., 1995; Bustamante & Rivetti, 1996) are paradigmatic of this problem. In the latter case, the surface adsorption may affect both the mean and the width of the bend angle distribution (unpublished results).

In this study, DNA molecules deposited onto mica were imaged in air by SFM and their shape was analyzed using polymer chain statistics. DNA has the advantage that its equilibrium chain parameters, such as the mean-square end-to-end distance, $\langle R^2 \rangle$, and the mean-square bend angle between two chain segments, $\langle \theta^2 \rangle$, have been theoretically described in both two-dimensional and three-dimensional cases (Kratky & Porod, 1949; Flory, 1969; Schellman, 1974; Landau & Lifschitz, 1980).

To investigate the mechanism through which DNA molecules are transported from the deposition drop to the surface, the DNA concentration on the surface was determined as a function of the deposition time. This made it possible to control the number of DNA molecules per unit area and to determine an optimal deposition time for a given DNA concentration.

Theory

Molecular deposition

If the transfer process from solution onto the substrate is governed solely by diffusion, the fraction of DNA molecules bound to the surface at any time t is approximately given by (Lang & Coates, 1968):

$$\frac{n_F(t)}{n_0} = \sqrt{\frac{4D}{\pi}}\sqrt{t} \tag{1}$$

where $n_F(t)$ is the number of molecules on the surface (molecules per cm^2), n_0 is the total number of molecules in solution at $t = 0$ (molecules per cm^3), and D is the diffusion coefficient of the molecules. Equation (1) is valid if: (1) the DNA molecules are irreversibly adsorbed to the substrate; (2) convection currents do not contribute to the transport of the molecules to the surface; and (3) the top layer of the deposition drop is not significantly depleted of DNA molecules during the time of deposition. If either condition (1) or (2) is not true, $n_F(t)/n_0$ will be proportional to a power of t higher than 0.5 (Lang & Coates, 1968).

Chain statistics

For a polymer molecule in two dimensions, the energy required to bend by an angle θ two segments located a distance ℓ apart is given by (Landau & Lifshitz, 1986):

$$E = \frac{YI\theta^2}{2\ell} \tag{2}$$

where Y is the Young's modulus, and I is the area moment of inertia of the molecule. These macroscopic quantities can be related to the persistence length of the polymer, P (Landau & Lifshitz, 1980), by:

$$YI = k_B T P \tag{3}$$

Where k_B is the Boltzmann constant and T is the absolute temperature. From equations (2) and (3), the normalized probability distribution function for the bend angle θ is:

$$\mathscr{P}(\theta(\ell))_{2D} = \sqrt{\frac{P}{2\pi\ell}}\, e^{-\frac{P\theta^2}{2\ell}} \tag{4}$$

Consequently the odd moments of the distribution are all zero, whereas, the even moments are:

$$\langle\theta^2(\ell)\rangle_{2D} = \frac{\ell}{P} \tag{5}$$

$$\frac{\langle\theta^4(\ell)\rangle_{2D}}{\langle\theta^2(\ell)\rangle^2_{2D}} = 3 \tag{6}$$

The distribution function (4) can be used to determine the average cosine of the angle θ between segments of the polymer separated by a distance ℓ:

$$\langle\cos(\theta)\rangle_{2D} = \int_{-\infty}^{\infty} \mathscr{P}(\theta(\ell))\cos(\theta)d\theta = e^{-\frac{\ell}{2P}} \tag{7}$$

Equation (7) shows that the average cosine of the angle between two segments in the polymer decreases exponentially with the separation, ℓ. Equation (7) also shows that the persistence length, P, is the decay length through which the memory of the initial orientation of the molecule persists. As indicated by equation (3), the persistence length is, in general, a function of the temperature. Using equation (7), the mean-square end-to-end distance of the polymer is:

$$\langle R^2\rangle_{2D} = \int_0^L ds \int_0^L \langle \vec{u}(s) - \vec{u}(s')\rangle ds'$$

$$= \int_0^L ds \int_0^L \langle\cos(\theta(s) - \theta(s'))\rangle ds' \tag{8}$$

where $\vec{u}(s)$ is the unit tangent to the chain at position s. Replacing equation (7) in (8) and integrating gives:

$$\langle R^2\rangle_{2D} = 4PL\left(1 - \frac{2P}{L}\left(1 - e^{-\frac{L}{2P}}\right)\right) \tag{9}$$

For $L \to \infty$, $\langle R^2\rangle_{2D} = 4PL$.

In three dimensions the molecule can also bend in a direction perpendicular to the plane and the mean-square end-to-end distance is given by (Flory, 1969):

$$\langle R^2\rangle_{3D} = 2PL\left(1 - \frac{P}{L}\left(1 - e^{-\frac{L}{P}}\right)\right) \tag{10}$$

For $L \to \infty$, $\langle R^2\rangle_{3D} = 2PL$.

When a three-dimensional chain is projected onto the x-y plane, the mean-square of the projected end-to-end distance becomes:

$$\langle R^2\rangle_{proj.} = \langle R_x^2\rangle + \langle R_y^2\rangle = \frac{2}{3}\langle R^2\rangle_{3D} \tag{11}$$

For $L \to \infty$:

$$\langle R^2\rangle_{proj.} = \frac{1}{3}\langle R^2\rangle_{2D}$$

This difference in the $\langle R^2\rangle$ values will be used in the analysis of the data to distinguish between molecules that have equilibrated on the surface and molecules that have been trapped.

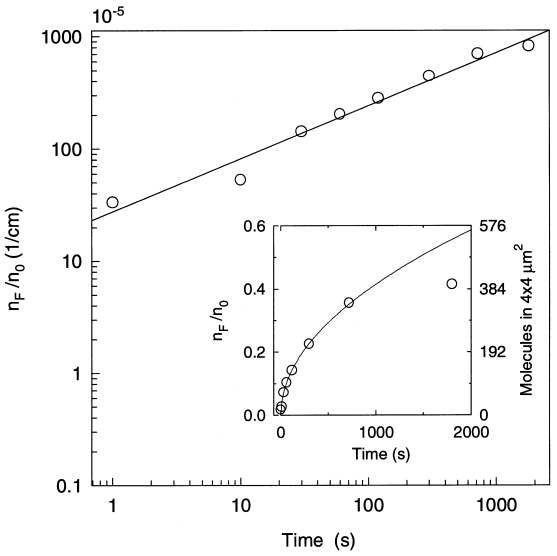

Figure 1. Ratio between the number of DNA molecules per cm^2 adsorbed on the surface, and the total number of molecules per cm^3 of the deposition drop plotted on a log-log scale as a function of time. The number of molecules per cm^2 were inferred from four 2 μm × 2 μm images. Only molecules that were more than half in the image frame were scored. The deposition drop, 20 μl of 0.5 nM DNA solution, contained a total of 6×10^9 DNA molecules (3×10^{11} molecules per cm^3). The slope of the regression line (continuous line) is 0.49 ± 0.04, and a diffusion coefficient $D = 5.5\ (\pm 2.1) \times 10^{-8}$ cm^2/s was calculated from the y-intercept.

In the insert, the data are plotted on a linear scale. The left y-axis represents the fraction of molecules bound to the surface with respect to the total number of molecules in the 20 μl drop. The right y-axis represents the actual number of molecules counted in a 4 μm × 4 μm area. The drop covered the whole mica disk (1 cm^2) with a thickness of approximately 200 μm. Thus, the maximum number of molecules that could have been adsorbed in a 4 μm × 4 μm area is approximately 960 molecules.

A diffusion coefficient $D = 5.4\ (\pm 0.2) \times 10^{-8}$ cm^2/s is obtained from the fitting to equation (1) (continuous line). In both plots, the data point at 30 minutes was not considered in the fitting because the top layer of the deposition drop is then depleted of about 15% of its DNA molecules and equation (1) no longer holds true (see Materials and Methods).

Results

DNA adsorption as a function of the deposition time

Aliquots (20 μl) of DNA stock solution (0.5 nM 1258 bp DNA fragment in buffer I) were deposited onto freshly cleaved mica. The samples were incubated for times varying from one second to 30 minutes. The deposition process was stopped by rinsing the sample with water and subsequent drying in a flow of nitrogen. The fraction of molecules bound to a 16 μm × 16 μm area was determined from the images at each time-point.

Figure 1 shows a log-log plot of the fraction of molecules adsorbed (normalized to 1/cm) *versus*

Table 1. DNA contour length measurements

DNA length (bp)	DNA length[a] (nm)	μ (nm)	σ (nm)	No. molecules
350	118.3	110.0	12.7	479
400	135.2	123.3	11.2	439
565	191.0	177.6	12.3	623
681	230.2	213.0	12.7	338
825	278.9	251.9	21.5	390
1258	425.2	388.6	22.4	378
2712	916.7	868.2	78.2	341
5994	2026.0	1856.2	102.5	928

[a] The DNA contour length was calculated from the number of base-pairs (0.338 nm/bp). μ and σ are the mean and the standard deviation of the DNA contour length distribution, as measured from the SFM images. For the 5994 bp DNA fragment, only molecules with a contour length greater than 1500 nm and less than 2200 nm were considered (96% of the total).

the deposition time t. The slope of the graph represents the power of t (see equation (1)) and is equal to 0.49 ± 0.04, in good agreement with the theoretical value of 0.5. A diffusion coefficient $D = 5.5\ (\pm 2.1) \times 10^{-8}\ \mathrm{cm^2/second}$ is obtained from the y-axis intercept of the plot in Figure 1, while a value of $D = 5.4\ (\pm 0.2) \times 10^{-8}\ \mathrm{cm^2/second}$ results from the fitting of the data to equation (1); see Figure 1, inset. Both values compare well with the semi-theoretical value $D_\theta = 5.4 \times 10^{-8}\ \mathrm{cm^2/second}$ (see Materials and Methods). The 30 minute time-point was excluded from the evaluation because the top layer of the deposition drop was significantly depleted of its DNA contents and, therefore, equation (1) is no longer valid (see Materials and Methods). These results suggest that the deposition process is solely diffusion-controlled, and that the molecules are irreversibly adsorbed onto the substrate.

The deposition process was also analyzed by varying the DNA concentration in the deposition drop between 0.5 and 10 nM (data not shown). The depositions were done in buffer I and stopped after 120 seconds by rinsing and drying the mica surface. In the range of 0.5 to 5 nM DNA, the number of molecules on the surface increased linearly from seven to about 70 molecules per μm^2. For higher concentrations of DNA, a deviation from linearity was observed, probably caused by saturation of the surface binding sites. All subsequent experiments were done at a low to medium surface coverage.

Analysis of the DNA end-to-end distance distributions

The average contour length values of eight different DNA fragments measured from the SFM images are reported in Table 1. More than 300 molecules for each fragment size were analyzed (the total number of molecules measured was 3916). All molecules fully contained in the image frame were included in the analysis. The mean contour length values (column 2 in Table 1) are about 8% shorter than the expected values assuming B-form DNA (column 3 in Table 1). Two facts can

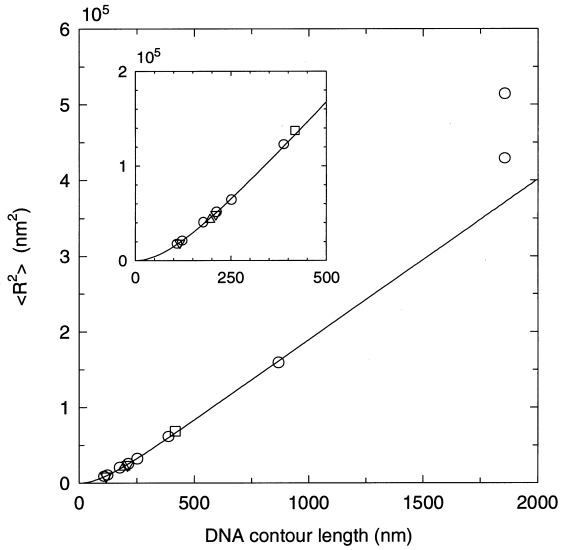

Figure 2. Mean-square end-to-end distance, $\langle R^2 \rangle$, as a function of the DNA contour length. The open symbols represent the $\langle R^2 \rangle$ values of the eight DNA fragments in different buffer conditions. Open circles, 4 mM Hepes (pH 7.4), 10 mM NaCl, 2 mM $MgCl_2$ (buffer I). Open squares, 4 mM Hepes (pH 7.4), 10 mM NaCl, 100 mM $MgCl_2$. Open triangles, 10 mM Hepes (pH 8.0), 80 mM NaCl, 5 mM $MgCl_2$. Open inverted triangles, 10 mM Hepes (pH 6.8 and 8.0); 5 mM NaCl, 5 mM $MgCl_2$. The abscissa values are the mean contour lengths of each DNA fragment as measured from the SFM images (Table 1). In all cases the DNA deposition was carried out at 23°C with an incubation time of about two minutes. For the 5994 bp fragment incubation times of one minute (lower point), five and ten minutes (higher superimposed points) were used. The continuous line represents the $\langle R^2 \rangle$ evaluated from equation (9) assuming a DNA persistence length of 53 nm. The insert is an expansion of the first part of the curve.

contribute to the reduction of the measured DNA contour length. (1) In a typical image one pixel corresponds to ~ 4 nm of DNA (12 bp) (512×512 pixels, scan size: 2000 nm). Therefore, DNA bends within this range cannot be resolved. (2) The smoothing procedure applied to the DNA contour coordinates utilizes polynomial fitting that systematically rounds sharp bends of the DNA trace. The drift of the piezoelectric tube while imaging contributes to the spread of the length distributions (column 4 in Table 1). The average height and width of the DNA polymer, as measured from the SFM images, were 0.55 ± 0.15 nm and 12 ± 3 nm, respectively. Both values are different from the known DNA diameter (2 nm). The reduced DNA thickness could result from sample compliance, differential interaction between the tip and the sample and between the tip and the mica surface, or both (Bustamante *et al*., 1993, 1994a). The increased DNA width is due to the broadening effect produced by the SFM tip (Bustamante *et al*., 1993).

Figure 2 is a plot of the mean-square end-to-end distance $\langle R^2 \rangle$ *versus* the measured contour length,

Table 2. Mean-square end-to-end distance of 1258 bp DNA fragments deposited onto mica with different procedures

Theoretical model			$\langle R^2 \rangle$ (nm^2)	Trapping	
Ideal worm-like chains in 3D			35,600[a]		
Ideal worm-like chains 2D			60,500[b]	No	
Orthogonal 3D → 2D projection			23,700[c]	Yes	
Surface treatment	Time	Rinse			No. of molecules
None		No	61,300	No	378
Glow-discharge	10 s	No	26,000	Yes	696
Water	12 h	Yes	25,100	Yes	752
$MgCl_2$, 10 mM	12 h	Yes	54,700	No	490
KCl, 10 mM	12 h	Yes	20,800	Yes	602
LiCl, 10 mM	12 h	Yes	32,900	Yes	500
LiCl, 10 mM	12 h	No	22,600	Yes	526
4 mM Hepes (pH 7.4), 10 mM NaCl, 2 mM $MgCl_2$	4 min	Yes	59,500	No	725
4 mM Hepes (pH 7.4) 10 mM NaCl	4 min	Yes	28,500	Yes	1493
NaCl, 10 mM	4 min	Yes	27,800	Yes	342
NaCl, 10 mM	4 min	No	61,100	No	700

The theoretical $\langle R^2 \rangle$ values were calculated from equations (10)[a], (9)[b] and (11)[c] using the measured contour length $L = 388.6$ nm and a DNA persistence length $P = 53$ nm. All $\langle R^2 \rangle$ values were rounded to the nearest 100 nm^2.

L, for the eight DNA samples used in this study (open symbols). Most depositions were done in buffer I, but a few depositions were done in other buffers (see the Figure legend). All the buffers contained Mg^{2+}, which is necessary to bind DNA to the surface (Bustamante *et al*., 1992; Vesenka *et al*., 1992). The experimental results in Figure 2 are compared with the theoretical $\langle R^2 \rangle$ values predicted by equation (9) (continuous line) assuming a persistence length of 53 nm (Bustamante *et al*., 1994b). The agreement between data and theory is excellent for DNA fragments shorter than 1000 nm (about 3000 bp), which suggests that DNA molecules deposited in these conditions are thermodynamically equilibrated in two dimensions before they are immobilized on the mica. The fitting of the data (for $L < 1000$ nm) to equation (9) gives a persistence length value of 52.3 ± 0.3 nm. If the calculated DNA contour length (0.338 nm/bp) is used instead of the measured contour length, the same fitting gives a persistence length value of 48 ± 0.7 nm.

Molecules of the 5994 bp DNA fragment were deposited with three different incubation times: one, five and ten minutes. In all cases, the measured $\langle R^2 \rangle$ was larger than the theoretical values predicted by equation (9). These larger values may be a manifestation of excluded volume effects that become increasingly important for larger molecules in two dimensions (Frontali, 1988; Grosberg & Khokhlov, 1994). The shorter value observed for the one minute deposition ($\langle R^2 \rangle = 4.29 \times 10^5$ nm^2, 126 molecules) with regard to the five and ten minute depositions ($\langle R^2 \rangle = 5.14 \times 10^5$ nm^2, 624 and 178 molecules, respectively) suggests that the equilibration time for such long polymers is of the order of minutes.

Table 2 reports the results obtained from a series of experiments in which DNA molecules were deposited onto mica treated with different procedures. The experimentally measured $\langle R^2 \rangle$ values are compared with the theoretical values determined for polymers in two dimensions.

DNA molecules deposited onto untreated, freshly cleaved mica are able to equilibrate on the surface. Qualitatively, the molecules appear extended with very few cross-overs even when the surface is crowded (Figure 3a). On the other hand, when DNA is deposited on glow-discharged mica (Figure 3b) or water-treated (H^+-exchanged) mica (Figure 3c), the molecules appear condensed, with a considerable number of cross-overs. In these cases, the mean-square end-to-end distance $\langle R^2 \rangle$ is much smaller than the theoretical $\langle R^2 \rangle_{2D}$ as determined by equation (9). Instead, it is close to the value predicted for molecules existing in three dimensions and orthogonally projected onto the surface plane (equation (11)). Therefore, DNA molecules deposited on such treated mica do not equilibrate on the surface, but are trapped immediately upon contact. It has been shown that the metal ions, which occupy the cavities formed by the oxygen atoms of the mica basal plane, are displaced in water-treated mica (Nishimura *et al*., 1994). It is possible that the observed kinetic trapping is due to the increased negative surface charge resulting from this exchange.

To further investigate the trapping effect, mica was treated with different salt solutions. The presence of $MgCl_2$ in the treatment solution prevented the trapping phenomenon even when the mica was extensively rinsed with water after the treatment. This finding is consistent with the observation that Mg^{2+} can bind tightly to the mica cavities and reduces the negative surface charge density. Conversely, overnight treatment with KCl or LiCl solutions did not prevent trapping of the molecules. Presumably, at least with the salt concentration used here, neither the hydrated K^+ or Li^+ can enter the mica binding sites. NaCl treatment

of shorter duration (Table 2, lower part) shows that DNA molecules are trapped on the surface only if the mica is rinsed with water after the treatment. This indicates that the mica surface is not modified by the presence of the monovalent salt, but by the water rinse that produces H^+-exchanged mica.

Analysis of the bend angle θ(ℓ) distribution

Figure 4a to f shows the plots of the ratio between the fourth moment and the square of the second moment for the θ distribution, as a function of the distance ℓ (equation (6)) between two chain vectors. The data were determined for six of the eight DNA molecules deposited in buffer I (open circles). In each case, the experimental data are close to the theoretical value of 3, indicating that the angle distribution is Gaussian, as is expected only for DNA molecules that have equilibrated in two dimensions. However, some deviation from the theoretical value is observed for very short ℓ, and for ℓ approaching the DNA contour length L.

The discrepancy observed for short ℓ values is likely caused by the finite pixel size of the images. To verify this hypothesis, worm-like chains were mathematically generated in a two-dimensional space (see Materials and Methods). The coordinates (in nm) of each segment were fitted with an integer grid of 512 × 512 pixels (SFM image size), converted back to a nanometer scale and smoothed as done for the experimental data. The ratio of the even moments of the θ-distribution (equation (6)) obtained from the simulated polymers is plotted in Figure 4d (filled circles). The graphs for the real and simulated molecules show the same behavior, confirming the interpretation given above. The deviation for ℓ approaching the contour length L could reflect the paucity of data points at the extreme end of each molecule. The reduced accuracy of the smoothing procedure applied to the DNA coordinates for points close to both ends of the molecules may also contribute to this effect. Hence, data points near both ends of the molecule were discarded in subsequent calculations.

Figure 5 shows a plot of the standard deviation of the angle distribution $\langle\theta^2(\ell)\rangle$ between two segments, as a function of their distance ℓ, for six DNA fragments of different length. The persistence length for each fragment is determined from the inverse of the regression slope of the plots (see equation (5)). DNA fragments unaffected by excluded volume interactions ($L < 2712$ bp, 917 nm) have a mean persistence length of 53.6 ± 1 nm, which agrees with the value obtained from the $\langle R^2\rangle$ analysis. For longer DNA molecules ($L > 2712$ bp, 917 nm), excluded volume effects become relevant, and the slope of the graph decreases with increasing contour length.

Excluded volume effects

Excluded volume effects resulting from the interaction among different molecules or among segments of the same molecule (self-avoiding effects) perturb the chain dimensions. Excluded volume effects increase with the length of the polymer, the DNA concentration, and the transfer from three to two dimensions (Joanicot & Revet, 1987). Because of their global nature, excluded volume effects cannot modify local properties like bending rigidity (persistence length). However, excluded volume effects alter the conformation of the polymer (i.e. $\langle R^2\rangle$ increases) and a misinterpretation of the data could result in an over-estimation of the persistence length. In this section, the effect of the excluded volume interactions on both $\langle R^2\rangle$ and $\langle\theta^2\rangle$ is analyzed. The term ''measured persistence length'' is used to indicate that the DNA persistence length was determined neglecting the excluded volume effects. Although, this

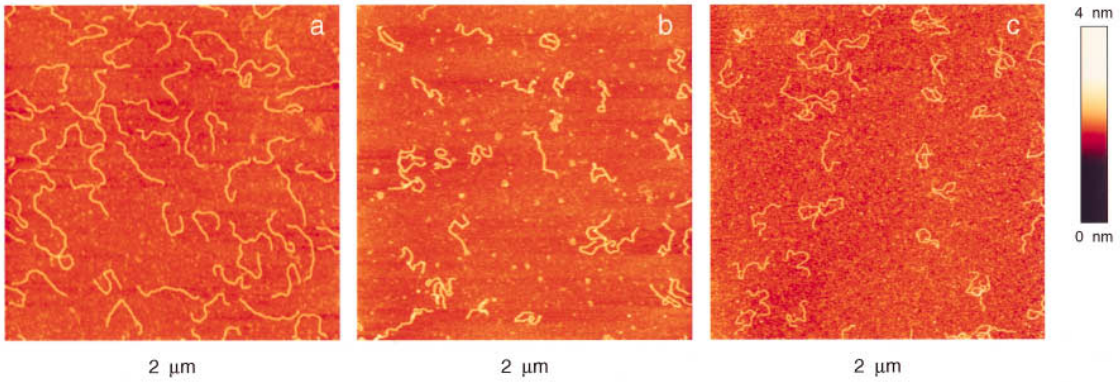

Figure 3. SFM images of the 1258 bp DNA fragment deposited on mica with three different deposition methods. a, An aliquot (20 µl) of 1 nM DNA solution in buffer I was deposited onto freshly cleaved mica and incubated for two minutes. b, An aliquot (20 µl) of 0.5 nM DNA solution in buffer I was deposited onto glow-discharged mica and incubated for about one minute. c, An aliquot (20 µl) of 1 nM DNA solution was deposited onto H^+-exchanged mica obtained by soaking the mica disk in water for 12 hours. Qualitatively, the molecules on treated mica (b and c) appear more condensed than those on untreated mica (a). The SFM images (512 × 512 pixels) were collected in air with the tapping mode using a commercial silicon tip. The scan rate was about three lines per second. The $\langle R^2\rangle$ values of these molecules are reported in Table 2.

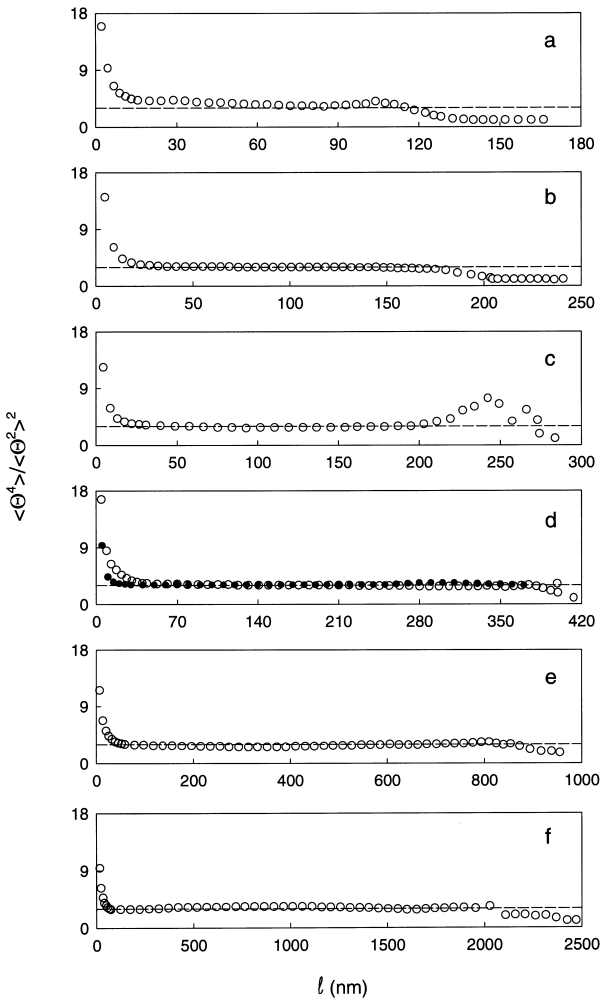

Figure 4. Ratio of the fourth moment and the square of the second moment of the θ distribution (equation (6)) for six DNA fragments deposited in buffer I: a, 350 bp; b, 565 bp; c, 825 bp; d, 1258 bp; e, 2712 bp; f, 5994 bp. θ is the angle between two segments separated by a distance ℓ along the DNA contour. In the central portion of all graphs, the ratio determined from the experimental data (open symbols) is very close to the theoretical value of 3 (broken line). At the two extremes, it deviates somewhat from 3 for reasons given in the text. The filled symbols in d correspond to simulated polymers that have been pixelized as described in the text.

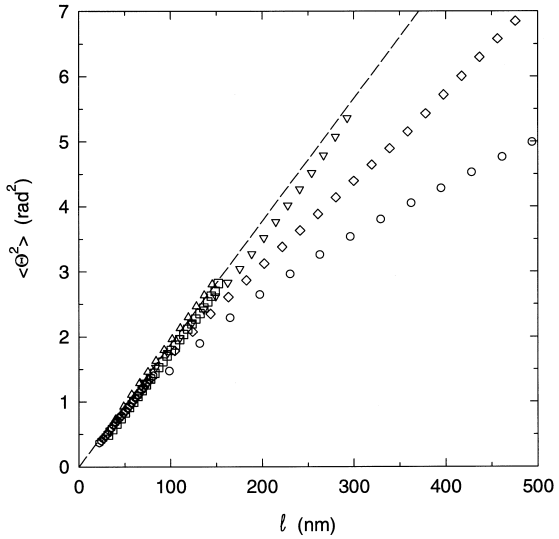

Figure 5. $\langle\theta^2\rangle$ as a function of the segment separation ℓ for the same DNA fragments as in Figure 4. Only ℓ values for which the ratio of the fourth moment and the square of the second moment of the θ-distribution was close to 3 (indicative of a Gaussian distribution) were considered in the evaluation. The persistence length is obtained from the inverse slope of the linear regressions. Open hexagons, 350 bp, P = 55.9 nm, ℓ range 20 to 80 nm; open squares, 565 bp, P = 51.7 nm, ℓ range 30 to 150 nm; open triangles, 825 bp, P = 51.7 nm, ℓ range 30 to 150 nm; open inverted triangles, 1258 bp, P = 55.1 nm, ℓ range 70 to 300 nm; open diamonds, 2712 bp, P = 71.1 nm, ℓ range 100 to 700 nm; open circles, 5994 bp, P = 146.7 nm, ℓ range 250 to 1500 nm. The slope of the broken line corresponds to P = 53 nm.

analysis is, in principle, not valid, the comparison of the measured persistence length between molecules which are and which are not affected by excluded volume effects illustrates well the relevance of excluded volume interactions for DNA molecules constrained in two dimensions.

The onset of the self-avoiding effects can be seen in Figure 5 where the measured persistence lengths of the 2712 bp and the 5994 bp fragments increase from 53 nm to 71 nm and 147 nm, respectively. To confirm this interpretation of the data, worm-like chains were mathematically generated in two dimensions, with and without excluded volume effects, using Monte Carlo methods. A detailed description of the simulation procedure is given in Materials and Methods. In Figure 6, an experimental image is compared with the images generated from the simulation. Qualitatively, the DNA molecules (Figure 6a) appear similar to the simulated polymers when excluded volume effects are taken into account (Figure 6b). In contrast, they are markedly different from the polymers simulated without excluded volume effects (Figure 6c). As already mentioned, DNA molecules imaged by SFM seldom cross themselves or other molecules even when the surface is crowded with DNA.

Figure 7a shows the mean-square end-to-end distance *versus* the contour length of chains simulated with (filled triangles) and without (filled circles) excluded volume effects. The theoretical mean-square end-to-end distance determined by equation (9) (continuous line), and representative data points of DNA molecules deposited in buffer I (open circles) are also shown. The mean-square end-to-end distance of the simulated polymers shows that excluded volume interactions do not significantly perturb the chain dimensions of molecules with a contour length shorter than 1000 nm (~20 persistence lengths). However, for a polymer with a contour length of about 2000 nm, the $\langle R^2\rangle$ value is almost twice as large as that predicted for unperturbed chains.

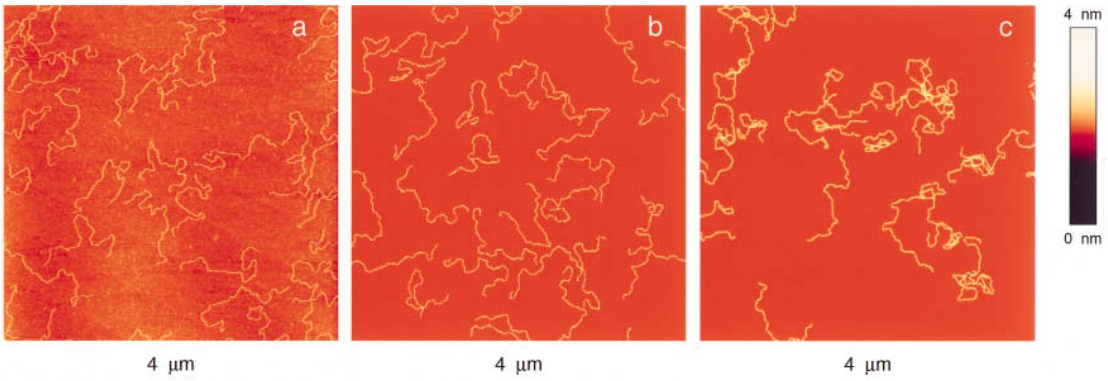

Figure 6. Images of DNA molecules and simulated worm-like chains in two dimensions. a, SFM image of the 5994 bp DNA fragment recorded in air with the tapping mode (contour length 1856.2 nm). The DNA was deposited onto freshly cleaved mica in buffer I with an incubation time of five minutes. b, Polymers simulated without excluded volume effects and (c) with excluded volume effects. In both cases the polymers were simulated in a 4 μm × 4 μm area with a contour length of 1855 nm (closest multiple of five to the mean DNA contour length measured from the SFM images). A persistence length of 53 nm was used. The images (b and c) were obtained by passing a hypothetical parabolic tip, with 10 nm radius of curvature, over the simulated polymers. The polymer was assumed to be 1 nm in height.

In Figure 7b, $\langle\theta^2\rangle$ of the 5994 bp DNA fragment is plotted *versus* the segment separation ℓ for DNA molecules (open circles) and simulated polymers (filled triangles). Three regions can be distinguished in the graphs: For small values of ℓ (less than 250 nm, region I), the measured DNA persistence length is about 60 nm for both DNA and simulated polymers. In this region, the distance between two segments of a molecule is too small for the self-avoiding interactions to affect the behavior of the molecule. For intermediate values of ℓ (250 to 1500 nm, region II), the measured persistence length increases to about 147 nm for DNA molecules and 274 nm for the simulated polymers. In this case the DNA appears stiffer due to the self-avoiding effects. Finally, for very long ℓ values (larger than 1500 nm, region III), the segments are so far apart that their relative orientation becomes uncorrelated, and the slope of the curves increases again. Interestingly, the two curves have similar shapes but, in the central portion (region II), their slopes are different in magnitude. This could be due to the constraints imposed by the simulation when generating molecules with excluded volume effects. The energy of interaction among different polymer segments was assumed to be extremely high and the molecule-surface interaction was not taken into account. Although the excluded volume effects make the DNA appear stiffer, the molecules still behave as ideal polymers in two dimensions with a Gaussian θ-distribution (Figure 4f).

Deposition of protein-end labeled DNA complexes

The data for DNA depositions on freshly cleaved mica strongly suggest that DNA molecules are able to equilibrate in two dimensions prior to their final attachment to the mica surface. The question remains of whether these results may be extrapolated to protein-DNA complexes, since protein-mica interactions may inhibit the equilibration of the complexes on the surface and could potentially distort their conformation. In general, this effect may depend on the type of protein and substrate, as well as on the buffer conditions of the deposition.

In an effort to further analyze the protein-mica interactions, streptavidin-horseradish peroxidase fusion protein (140 kDa, pI ≈ 6.5) was bound to both biotinylated ends of the DNA molecules. This protein was used instead of streptavidin because the greater molecular mass facilitates its recognition under the microscope (Figure 8). A strong protein-surface interaction will prevent equilibration of the complexes in two dimensions. Therefore, as in the case of glow-discharged mica, the mean-square end-to-end distance value of such complexes should be much smaller than that of DNA molecules equilibrated in two dimensions. Conversely, if the protein-surface interaction is weak, the mean-square end-to-end distance of the complexes will be comparable with that of free DNA molecules.

End-labeled DNA fragments of three different lengths were deposited onto freshly cleaved mica in 4 mM Hepes (pH 7.4), 23 mM NaCl, 4 mM $MgCl_2$ and allowed to settle for about three minutes before rinsing and drying. Figure 8 shows that approximately 90% of the DNA molecules have a protein bound to both ends. Table 3 shows the $\langle R^2\rangle$ values obtained from the end-labeled DNA fragments and compares them with the theoretical values calculated using equation (9). None of the $\langle R^2\rangle$ values is smaller than those predicted from the equilibration model in two dimensions, which suggests that streptavidin end-labeled DNA can still equilibrate on the surface. It is not clear whether the difference between the theoretical and the experimental $\langle R^2\rangle$ values is significant. Since the deviation increases with the DNA contour length, it may be due to self-avoiding effects.

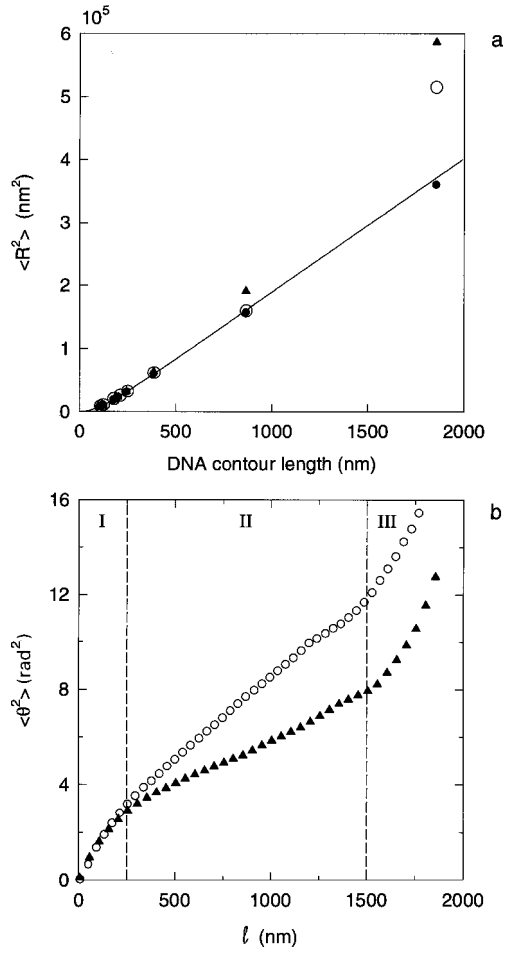

Figure 7. Comparison of the chain parameters obtained from real and simulated DNA molecules. a, Open circles, $\langle R^2 \rangle$ values of real DNA molecules (see also Figure 2). Filled circles $\langle R^2 \rangle$ values of simulated polymers without excluded volume effects. Filled triangles, $\langle R^2 \rangle$ values of simulated polymers with excluded volume effects. One thousand polymers for each of the eight contour lengths were simulated. Also plotted is equation (9) assuming a persistence length $P = 53$ nm (continuous line). b, Open circles, $\langle \theta^2 \rangle$ of real DNA molecules (5994 bp, mean contour length 1856.2 nm). Filled triangles, $\langle \theta^2 \rangle$ of simulated polymers (contour length, 1855 nm), with excluded volume effects. Three regions with a significantly different slope can be distinguished in the plot. I, The measured persistence length, as determined from the inverse of the slope, is about 60 nm in both cases. II, The measured persistence length is 147 nm and 274 nm for the real DNA molecules and the simulated polymers, respectively. III, The slope of the curves increases as a result of the fading correlation between the segments as ℓ becomes large.

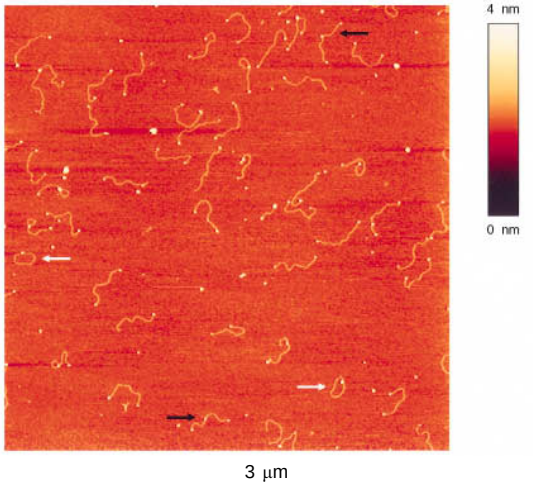

Figure 8. SFM image of DNA fragments end-labeled with the streptavidin-horseradish peroxidase fusion protein. A 20 μl drop containing the complexes at a concentration of 0.5 nM DNA (1048 bp) was deposited on freshly cleaved mica in a low-salt buffer (4 mM Hepes (pH 7.4), 23 mM NaCl, 4 mM $MgCl_2$). The deposition drop was incubated on the mica disk for three minutes before it was rinsed with water then dried with nitrogen. When measuring the end-to-end distances, complexes with a looped structure (white arrows) or with proteins bound along the DNA (black arrow) were not considered. The SFM image (512x512 pixels) was collected in air with the tapping mode using a commercial silicon tip. The scan rate was about three lines per second.

Discussion

The transition from three dimensions (solution) to two dimensions (surface) alters the conformation of molecules, notably long polymers such as DNA. To interpret and quantitatively analyze SFM images of DNA and protein-DNA complexes, it is imperative to determine how the adsorption on the surface modifies the conformation of the molecules. DNA was chosen in this study for its biological importance and because adequate statistical treatments based on the worm-like chain model exist in two and three dimensions. (Kratky & Porod, 1949; Flory, 1969; Schellman, 1974; Frontali *et al*., 1979; Bettini *et al*., 1980; Landau & Lifschitz, 1980).

The kinetics of DNA adsorption on the surface shows that the number of molecules bound to the surface is proportional to the square-root of the deposition time t. This result, and the finding that the diffusion coefficient is comparable with that obtained in other studies (Crothers & Zimm, 1965), indicates that the DNA molecules are transported to the surface solely through diffusion, and once on the surface they cannot return into solution. Previous EM experiments (Lang & Coates, 1968) have reported similar results for DNA from bacteriophages T3 and χ.

The analysis of $\langle R^2 \rangle$ and $\langle \theta^2 \rangle$ values reveals that DNA molecules deposited in low salt solutions onto freshly cleaved mica do equilibrate on the surface and that short polymers (less than 20 persistence lengths) behave as ideal worm-like chains in two dimensions, with a persistence length of 53 nm. For longer polymers, self-avoiding effects become relevant and the statistical parameters deviate from the theoretical values.

The mean-square end-to-end distance value of protein-end labeled DNA fragments deposited onto

freshly cleaved mica shows that those complexes are also able to equilibrate on the surface, despite the additional protein-surface interaction. This finding cannot be extended to other DNA-binding proteins but suggests that conditions that favor equilibration of protein-nucleic acid complexes may be found.

The DNA persistence length determined from the $\langle R^2 \rangle$ and $\langle \theta^2 \rangle$ data (52.5 ± 0.4 nm and 53.6 ± 1 nm, respectively) is in very good agreement with values obtained by independent methods (Hagerman, 1988; Porschke, 1991; Bustamante *et al*., 1994b; Bednar *et al*., 1995). The measurement of the DNA persistence length through direct visualization of the molecules possesses several advantages (Hagerman, 1988). DNA aggregation and molecular weight heterogeneity are eliminated. The measurements can be performed over a wide range of salt conditions. The persistence lengths of different regions of the molecule can be determined, and only a few femtomoles of DNA are required for one experiment. Moreover, DNA can be imaged in liquids by SFM, and the solution can be exchanged during imaging (Bustamante *et al*., 1994a; Bustamante & Keller, 1995). The only requirement for both EM and SFM is that the deposition and the interaction with the surface should alter the statistical parameter of the chain in a predictable manner. As described here, DNA molecules deposited onto freshly cleaved mica fulfil this requirement. In theory, useful information might be obtained also from molecules that are truly projected onto the surface. However, real DNA molecules kinetically trapped on the surface will deviate from their mathematical projection because, in the deposition process, the contour length must be conserved.

It has also been shown that, in 2D, excluded volume effects significantly alter the chain dimensions of DNA molecules longer than ~ 20 persistence lengths. Therefore, they must be taken into account when analyzing long polymers.

What are the molecular events that result in the transfer of DNA molecules from the solution to the surface and their equilibration in two dimensions? The square-root time-dependence of the kinetics of deposition indicates that DNA molecules simply diffuse from the solution to the surface, and once on the surface they remain bound to it. At first, this observation seems to be at odds with the thermal equilibration as evidenced by the statistical parameters of the molecules on the surface. However, these facts can be reconciled assuming that before the blotting step, the molecules, although irreversibly bound to the surface, are able to diffuse laterally and interconvert among the conformations accessible to them in two dimensions. Evidence of lateral diffusion of DNA molecules deposited onto mica and imaged in liquid has been obtained from SFM studies (Bezanilla *et al*., 1994; unpublished results). Presumably, it is this equilibrated population of molecules on the surface that is fixed in place during the blotting step of the deposition.

These ideas suggest a model in which the mica surface can be described as a discrete array of binding sites capable of interacting with the polymer segments. In reality, the mica binding sites may correspond to the hexagonal cavities formed by the oxygen atoms of the mica basal plane. The DNA segments may correlate to the Mg^{2+} bound to the phosphate backbone. In this model, the dynamics of the molecules on the surface are controlled by the density of binding sites and the strength of the polymer-binding site interaction.

Specifically, the equilibration time of a polymer molecule lying on the surface is determined by the time the molecule requires to sample among its accessible configurations in two dimensions. Let us assume that a polymer molecule is made up of N identical units that interact with the surface independently. If ν is the number of degrees of freedom for a single unit, in the absence of excluded volume effects, each polymer can exist in ν^N independent configurations on the surface. Denoting with ρ_0 the transition rate of one unit among its degrees of freedom, in the absence of binding interactions with the surface, then the average time required by a polymer molecule to sample its accessible configurations can be written as:

$$t_{N,0} \sim \frac{\nu^N}{N\rho_0} \tag{12}$$

Table 3. Theoretical and experimental $\langle R^2 \rangle$ values of protein-end labeled DNA fragments with different contour length

DNA length (bp)	No. molecules	$L_{calc.}$ (nm)	$L_{meas.}$ (nm)	$\langle R^2 \rangle_{theor.}$ (nm^2)	$\langle R^2 \rangle_{meas.}$ (nm^2)
1048	499	354.2	354.2	53,400	54,400
1801	219	608.7	551.9	94,700	120,000
2763	287	933.9	889.5	166,000	225,000

$L_{calc.}$ is the DNA contour length determined from the number of base-pairs (0.338 nm/bp). $L_{meas.}$ is the mean DNA contour length measured from the SFM images. $\langle R^2 \rangle_{theor.}$ is the mean-square end-to-end distance as calculated from equation (9) using a DNA contour length as reported in column 4 and a DNA persistence length of 53 nm. $\langle R^2 \rangle_{meas.}$ is the mean-square end-to-end distance measured from the SFM images. Looped complexes or complexes in which a protein was bound along the length of the DNA were not considered in the measurement. All $\langle R^2 \rangle$ values were rounded to the nearest 100 nm^2.

In the presence of binding interactions, the fraction of polymer units bound to the surface at any given time after equilibration has occurred is:

$$f_b = \frac{\sigma K_b}{1 + \sigma K_b} \quad (13)$$

where K_b is the binding constant of a polymer unit at a surface binding site, and σ is the fraction of the surface (surface density) containing binding sites. For such molecules, the average rate of transition of a polymer unit among its degrees of freedom is, at equilibrium:

$$\rho_{average} = f_b \rho_b + (1 - f_b)\rho_0 \quad (14)$$

where $\rho_b = \rho_0 e^{-E_a/k_B T}$ represents the transition rate for a bound polymer unit assuming a simple two-state process. E_a is the activation energy required to break a binding site polymer unit interaction on the surface, k_B is the Boltzmann constant and T the absolute temperature. Substituting ρ_b into equation (14) and combining equations (12), (14) and (13), the equilibration time for polymer molecules interacting with discrete sites on the surface becomes:

$$t_N = \frac{\nu^N}{N\rho_{average}} = \frac{\nu^N}{N\rho_0\left[1 - \frac{\sigma K_b}{1 + \sigma K_b}\left(1 - e^{-\frac{E_a}{k_B T}}\right)\right]} \quad (15)$$

Equation (15) describes several aspects of the equilibration process on the surface. The equilibration time increases with the polymer length. In fact, the time required to reach a stable $\langle R^2 \rangle$ value for the 5994 bp DNA fragment was about five minutes, whereas the shorter fragments were equilibrated in less than one minute. The equilibration time also increases with the energy of activation needed to break a surface-polymer bond, and with the density of binding sites on the surface, σ. In addition, equation (15) shows that if $E_a \approx k_B T$, the molecules will be able to equilibrate and even diffuse laterally on the surface. The magnitude of E_a is determined by the binding energy of a polymer unit to the binding site ($k_B T \ln(K_b)$) and the average distance between adjacent sites on the surface. Clearly, even if the polymer can diffuse on the surface, it may remain irreversibly bound to it if $NE_a \gg k_B T$.

Based on this model, the DNA trapping effect described above, can be rationalized as follows. DNA binding to mica is very likely mediated by magnesium ions that bridge between the negative charges of the phosphate backbone and the negative mica sites. It has also been shown that magnesium ions can enter the hexagonal cavities formed by the basal oxygen atoms of the mica layer (Nishimura *et al*., 1995). Glow-discharging the mica results in an increased negative charge density on the surface (Namork & Johansen, 1982). The same effect is obtained by soaking the mica in or rinsing it with de-ionized water, since the metal ions are displaced from the negative mica binding sites (Nishimura *et al*., 1994). Therefore, DNA molecules deposited on glow-discharged or H^+-exchanged mica may be trapped on the surface because of an increased energy of interaction between surface binding sites and DNA. Stronger binding will lead to higher activation energies preventing lateral diffusion and equilibration.

Conclusion

Eight DNA fragments of different contour lengths were deposited onto mica and imaged in air using SFM. It was shown that the DNA is transported to the surface solely by diffusion and it is irreversibly adsorbed. When deposited on untreated freshly cleaved mica, the DNA molecules equilibrate onto the surface as in an ideal two-dimensional solution. Glow-discharged or H^+-exchanged mica prevents DNA from freely equilibrating on the surface and the molecule conformation resembles a 3D projection onto the plane. Both experimental data and simulations of worm-like polymers show that excluded volume interactions affect the polymer conformation of DNA molecules longer than 20 persistence lengths. A protein attached to both ends of the DNA does not prevent the molecules from freely equilibrating on the surface during the deposition process. The $\langle R^2 \rangle$ values of such complexes are comparable with those of free DNA and to the theoretically predicted $\langle R^2 \rangle$ values. Under equilibrium conditions and in the absence of excluded volume effects, a DNA persistence length of 53 nm is measured. The deposition conditions described here should facilitate the reliable use of SFM, and other microscopy techniques that involve imaging molecules fixed to a substrate, to study the conformation of complex macromolecular assemblies.

Materials and Methods

Sample preparation

DNA fragments

The 350 bp DNA fragment was produced by PCR using pDE13 plasmid as template (Erie *et al*., 1993). The amplified region was between position 2183 and 2533. The 565 bp and the 825 bp fragments were obtained by *Nsp*I digestion of pDE13. The 400 bp fragment was obtained by PCR using pSFM1 as template. pSFM1 is a Bluescript KS^+ derivative (a gift from S. Hermann). The amplified region was between positions 932 and 1331. The 681 bp fragment was a gift from W. A. Rees. The 1258 bp fragment was obtained from a combined restriction digestion of pDE13 with *Pst*I and *Stu*I endonucleases. The 2712 bp and the 5994 bp fragments derive from the linearization with *Eco*RI of plasmid pNEB193 and plasmid pDE13, respectively. All the DNA fragments, with the exception of the last two, were gel-purified in a 1.5% (w/v) agarose gel and electroeluted by means of an Elutrap apparatus (Schleicher & Schuell, Keene NH). All the DNA fragments were purified by extraction with phenol/chloroform and precipitation in ethanol. The DNA pellet was resuspended in TE buffer

and the DNA concentration was determined from the absorption at 260 nm. All the restriction enzymes were purchased from Boehringer-Mannheim. pNEB193 plasmid was purchased from New England Biolabs. Concentrations of DNA are reported in units of nM molecules.

Protein-end labeled DNA

The 1048 bp, 1801 bp and 2763 bp fragments were obtained by a combined restriction digestion of pDE13 with *Ava*I and *Aha* endonucleases. The 5' overhangs were filled using the Klenow fragment of DNA polymerase I (New England Biolabs). The 1 ml reaction contained 50 μg of DNA, 50 units of Klenow enzyme, 33 μM dATP, 33 μM dGTP, 33 μM dTTP, 3.3 μM biotinylated-dCTP, 0.1 mg/ml bovine serum albumin and reaction buffer supplied with the enzyme. The reaction was incubated for 15 minutes at room temperature, then stopped by addition of 20 μl of 500 mM EDTA and heat inactivation at 75°C for ten minutes. The DNA was gel-purified, electroeluted and extracted as described above.

The streptavidin-horseradish peroxidase conjugate (Pierce, Rockford, IL) is a fusion protein consisting of 2 mol of peroxidase (40 kDa) per mole of streptavidin (60 kDa) for a total molecular mass of 140 kDa. An average isoelectric point of about 6.5 is calculated from the isoelectric points of the two proteins. Therefore, in the deposition buffer (pH 7.4) the protein is slightly negative. Streptavidin, and thus the conjugated protein, contains four biotin-binding sites. To prevent DNA looping, three of the biotin-binding sites were saturated with free biotin after the conjugated protein was loaded onto an immobilized Iminobiotin column (Pierce, Rockford, IL). Streptavidin binds strongly to iminobiotin at pH 11 but can be eluted at pH 4. For the mono-binding site protein preparation, the protocol reported in the product information sheet was followed. The column was washed with a 20 μM biotin solution in a low-salt buffer (binding buffer diluted 100 times). The eluted protein was dialyzed overnight against buffer I (4 mM Hepes (pH 7.4), 10 mM NaCl, 2 mM $MgCl_2$) and concentrated in a Centricon 50 (Amicon) to a final concentration of about 300 nM. The final NaCl concentration was adjusted to 100 mM. The DNA binding reaction was done in 4 mM Hepes (pH 7.4), 90 mM NaCl, 2 mM $MgCl_2$. By means of a protein titration, the optimal protein to DNA ratio was found to be 9, with a DNA concentration of about 20 nM. Under these conditions, about 90% of the DNA molecules were labeled at both ends and very few DNA loops were observed.

Sample deposition

Time-dependence of DNA adsorption to the mica

A 20 μl solution containing 0.5 nM of the 1258 bp DNA fragment in buffer I (4 mM Hepes (pH 7.4), 10 mM NaCl, 2 mM $MgCl_2$) were deposited onto freshly cleaved mica. The sample was incubated on the mica for varying times as indicated in the text. To prevent evaporation, the sample was kept in a sealed Petri dish containing an excess of buffer I. The sample was then rinsed with about 10 ml of water and excess liquid was blotted off with Whatman filter-paper before the mica was blown dry with nitrogen. All water was purified by distillation, followed by treatment in a Nanopure (Barnstead, Dubuque Iowa) water purification apparatus.

DNA depositions onto freshly cleaved mica

The deposition procedure was as described above except that DNA fragments of different length may have been used as indicated in the text. Unless otherwise stated, deposition times were usually one to two minutes, and the DNA concentration was between 0.5 and 2 nM. If a buffer other than buffer I was used, it is explicitly state in the Figure legend.

DNA depositions onto treated mica

Freshly cleaved mica was glow-discharged for ten seconds and 20 μl of 0.5 nM DNA solution were deposited for one minute. The surface was then rinsed with water and dried with a flow of dry nitrogen.

The overnight treatments were done by incubating the mica disk in 100 ml of water or 10 mM $MgCl_2$. After the surface was rinsed and dried, 20 μl of 1 nM DNA in buffer I were deposited for two minutes.

For the four minute treatment, 20 μl of the treatment solutions as (Table 2) were applied to the freshly cleaved mica, rinsed, when indicated, with water and dried with a flow of dry nitrogen before the DNA deposition. When the mica was not rinsed after the treatment, DNA in buffer I was deposited directly into the treatment solution. In all cases the rinsing was done by flushing 15 to 20 ml of water over the mica surface with a squirt bottle.

Scanning force microscopy

All SFM images were obtained in air at 23°C with a Nanoscope III microscope (Digital Instruments Inc., Santa Barbara, CA) operating in tapping mode. Commercial diving board silicon tips (Nanosensor, Digital Instruments) were used. The microscope was equipped with a type E scanner (12 μm × 12 μm). Freshly cleaved ruby mica (Mica New York, NY) was used as a substrate. The 512 × 512 pixels images were collected with a scan size between 2 and 4 μm at a scan-rate varying between two and five scan lines per second.

Image processing

The SFM images were analyzed using ALEX, an image analysis toolbox written locally in the Matlab environment (MathWorks Inc., Natick MA). The image integer values of the Nanoscope file were converted to nanometers using the relation given in the Nanoscope III documentation. The images were flattened by subtracting from each scan line the least-squares fitted polynomial with degree 2 or 3 depending on the image scan size. No additional filter was applied to the images.

The DNA path was digitized as follows. The two DNA ends and several points along the DNA contour were selected with the mouse. The points were then interpolated with one pixel steps. Around each pixel, the highest intensity in a given window (five to seven pixels wide) was sought. In this way, all the coordinates of the pixels with the highest value, corresponding to the DNA path, were found. To reduce the noise, the path was smoothed by polynomial fitting. For most of the images the distance between two consecutive points of the final DNA path was about 5 nm. The end-to-end distance was defined as the distance between the first and the last points of each DNA path. Measurements of the angle θ between two segments separated by a distance ℓ, was

done as described (Frontali *et al*., 1979). The contour length of DNA molecules deposited on glow-discharged or H^+-exchanged mica has not been measured because the path of molecules was often ambiguous. In these cases the calculated contour length (0.338 nm/bp) was used instead.

Monte Carlo simulation of a worm-like chain in two dimensions

The polymer model described by Schellman (1974) was used to generate worm-like polymers at equilibrium in a two-dimensional space. The polymers were simulated with and without taking into account excluded volume effects. In both cases the interaction energy between a polymer and the surface was assumed to be zero.

A simulated chain consisted of a series of n segments of length λ and infinitesimal thickness, joined together at one end. The angle θ between two consecutive segments was chosen by a Monte Carlo method from normally distributed numbers with mean zero and variance according to equation (5). The length λ of one segment was 5 nm and the polymer persistence length was set to 53 nm. The polymer contour length was the closest multiple of five to the mean of the DNA contour length measured from the images.

For chains without excluded volume effects, the interaction energy between two segments was taken to be zero. This implies that a newly generated segment is allowed to cross any other segment.

To simulate excluded volume effects, the interaction energy between two segments of the polymer was assumed to be very large. A growing chain was, therefore, discarded if it crossed itself or other chains already generated.

Determination of the diffusion coefficient

The diffusion coefficient D at temperature δ°C, is given by:

$$D = \frac{t_\delta \eta_{20;w}}{t_0 \eta_\delta} D_0$$

where $\eta_{20;w}$ and η_δ are the viscosities of water at the reference temperature $t_0 = 20$°C and at δ°C respectively. D_0 is the diffusion coefficient of DNA at the reference temperature, and is given by:

$$D_0 = \frac{8.218 \times 10^{-5} M^{0.445} + 0.0146}{M} \frac{\text{cm}^2}{\text{s}}$$

(Crothers & Zimm, 1965) where M is the molecular mass of the DNA.

Validity of the diffusion law

The fraction of DNA molecules left in the top layer of the deposition drop after a time t is given by:

$$\frac{n_{\text{top}}}{n_0} = erf\left(\frac{x_0}{2\sqrt{Dt}}\right)$$

(Lang & Coates, 1968) where *erf* is the error function and x_0 is the drop's thickness. According to this equation under the present experimental set-up (i.e. drop thickness ≈ 200 μm) the diffusion law is valid for up to 12 minutes, at which time the DNA concentration of the top layer of the drop is depleted by about 2%. After 30 minutes, it is depleted by 15%, which results in reduced DNA deposition on the surface.

Acknowledgements

We are grateful to Mark Young for a critical reading of the paper. We thank Chip Walker for providing some of the data. This work was supported by NSF grants MBC 9118482 and BIR 9318945 and NIH grant GM-32543. This work was supported in part by a grant from the Lucille P. Markey Foundation to the Institute of Molecular Biology. C.R. was supported by a Human Frontier Science Program (HFSP) long term fellowship.

References

Bednar, J., Furrer, P., Katritch, V., Stasiak, A. Z., Dubochet, J. & Stasiak, A. (1995). Determination of DNA persistence length by cryo-electron microscopy. Separation of the static and dynamic contributions to the apparent persistence length of DNA. *J. Mol. Biol.* **254**, 579–594.

Bettini, A., Pozzan, M. R., Valdevit, E. & Frontali, C. (1980). Microscopic persistence length of DNA: Its relation to average molecular dimensions. *Biopolymers,* **19**, 1689–1694.

Bezanilla, M., Drake, B., Nudler, E., Kashlev, M., Hansma, P. K. & Hansma, H. G. (1994). Motion and enzymatic degradation of DNA in the atomic force microscope. *Biophys. J.* **67**, 2454–2459.

Binnig, G., Quate, C. F. & Gerber, C. H. (1986). Atomic force microscope. *Phys. Rev. Letters,* **56**, 930–933.

Bustamante, C. & Keller, D. (1995). Scanning force microscopy in biology. *Physics Today,* **48**, 32–38.

Bustamante, C. & Rivetti, C. (1996). Visualizing protein-nucleic acid interactions on a large scale with the scanning force microscope. *Annu. Rev. Biophys. Biomol. Struct.* **25**, 395–429.

Bustamante, C., Vesenka, J., Tang, C. L., Rees, W., Guthold, M. & Keller, R. (1992). Circular DNA molecules imaged in air by scanning force microscopy. *Biochemistry,* **3**, 22–26.

Bustamante, C., Keller, D. & Yang, G. (1993). Scanning force microscopy of nucleic acids and nucleoprotein assemblies. *Curr. Opin. Struct. Biol.* **3**, 363–372.

Bustamante, C., Erie, D. A. & Keller, D. (1994a). Biochemical and structural applications of scanning force microscopy. *Curr. Opin. Struct. Biol.* **4**, 750–760.

Bustamante, C., Marko, J. F., Siggia, E. D. & Smith, S. (1994b). Entropic elasticity of λ-phage DNA. *Science,* **265**, 1599–1600.

Crothers, D. M. & Zimm, B. H. (1965). Viscosity and sedimentation of the DNA from bacteriophages T2 and T7 and the relation to molecular weight. *J. Mol. Biol.* **12**, 525–536.

Erie, D. A., Hajiseyedjavadi, O., Young, M. C. & von Hippel, P. H. (1993). Multiple RNA polymerase conformations and GreA: control of the fidelity of transcription. *Science,* **262**, 867–873.

Erie, D. A., Yang, G., Schultz, H. C. & Bustamante, C. (1994). DNA bending by Cro protein in specific and nonspecific complexes: implications for protein site recognition and specificity. *Science,* **266**, 1562–1566.

Flory, P. J. (1969). *Statistical Mechanics of Chain Molecules*, Interscience Publishers, New York.

Frontali, C. (1988). Excluded-volume effect on the bidimensional conformation of DNA molecules adsorbed to protein films. *Biopolymers,* **27**, 1329–1331.
Frontali, C., Dore, E., Ferrauto, A., Gratton, E., Bettini, A., Porzzan, M. R. & Valdevit, E. (1979). An absolute method for the determination of the persistence length of native DNA from electron micrographs. *Biopolymers,* **18**, 1353–1373.
Griffith, J. D., Makhov, A., Zawel, L. & Reinberg, D. (1995). Visualization of TBP oligomers binding and bending the HIV-1 and adeno promoters. *J. Mol. Biol.* **246**, 576–584.
Grosberg, A. Y. & Khokhlov, A. R. (1994). *Statistical Physics of Macromolecules*, API Press, Woodbury, NY.
Hagerman, P. J. (1988). Flexibility of DNA. *Annu. Rev. Biophys. Biophys. Chem.* **17**, 265–286.
Hansma, H. G. & Hoh, J. (1994). Biomolecular imaging with atomic force microscope. *Annu. Rev. Biophys. Biomol. Struct.* **23**, 115–139.
Hansma, H. G., Browne, K. A., Bezanilla, M. & Bruice, T. C. (1994). Bending and straightening of DNA induced by the same ligand: characterization with the atomic force microscope. *Biochemestry,* **33**, 8436–8441.
Joanicot, M. & Revet, B. (1987). DNA conformational studies from electron microscopy. I. Excluded volume effect and structure dimensionality. *Biopolymers,* **26**, 315–326.
Kratky, O. & Porod, G. (1949). Röntgenuntersuchung aufgelöster Fadenmoleküle. *Recueil,* **68**, 1106–1122.
Landau, L. D. & Lifshitz, E. M. (1980). *Statistical Physics, Part 1*. 3rd edit, Pergamon Press, Oxford, NY.
Landau, L. D. & Lifshitz, E. M. (1986). *Theory of Elasticity*, Pergamon Press, Oxford, NY.
Lang, D. & Coates, P. (1968). Diffusion coefficient of DNA in solution at ''zero'' concentration as measured by electron microscopy. *J. Mol. Biol.* **36**, 137–151.
Lang, D., Bujard, H., Wolff, B. & Russell, D. (1967). Electron microscopy of size and shape of viral DNA in solutions of different ionic strengths. *J. Mol. Biol.* **23**, 163–181.
Lindsay, S. M., Tao, N. J., DeRose, J. A., Oden, P. I. & Lyubchenko, L. Y. (1992). Potentiostatic deposition of DNA for scanning probe microscopy. *Biophys. J.* **61**, 1570–1584.
Lyubchenko, L. Y., Lindsay, S. M., DeRose, J. A. & Thundat, T. (1991). A technique for stable adhesion of DNA to a modified graphite surface for imaging by scanning tunneling microscopy. *J. Vac. Sci. Technol.* **9**, 1288–1290.
Lyubchenko, Y. L., Shlyakhtenko, L. S., Harrington, R. E., Oden, P. I. & Lindsay, S. M. (1993). Atomic force microscopy of long DNA: imaging in air and under water. *Proc. Natl Acad. Sci. USA,* **90**, 2137–2140.
Namork, E. & Johansen, B. V. (1982). Surface activation of carbon film supports for biological electron microscopy. *Ultramicroscopy,* **7**, 321–330.
Nishimura, S., Biggs, S., Scales, P. J., Healy, T. W., Tsunematsu, K. & Tateyama, H. (1994). Molecular-scale structure of the cation modified muscovite mica basal plane. *Langmuir,* **10**, 4554–4559.
Nishimura, S., Scales, P. J., Tateyama, H., Tsunematsu, K. & Healy, T. W. (1995). Cationic modification of muscovite mica: an electrokinetic study. *Langmuir,* **11**, 291–295.
Porschke, D. (1991). Persistence length and bending dynamics of DNA from electrooptical measuraments at high salt concentrations. *Biophys. Chem.* **40**, 169–179.
Rabke, C. E., Wenzler, L. A. & Beebe, T. P. J. (1994). Electron spectroscopy and atomic force microscopy studies of DNA adsorption on mica. *Scanning Microsc.* **8**, 471–478.
Rees, W. A., Keller, R. W., Vesenka, J. P., Yang, G. & Bustamante, C. (1993). Evidence of DNA bending in transcription complexes imaged by scanning force microscopy. *Science,* **260**, 1646–1649.
Schaper, A., Pietrasanta, L. I. & Jovin, T. M. (1993). Scanning force microscopy of circular and linear plasmid DNA spread on mica with a quaternary ammonium salt. *Nucl. Acids Res.* **21**, 6004–6009.
Schellman, J. A. (1974). Flexibility of DNA. *Biopolymers,* **13**, 217–226.
Thundat, T., Allison, D. P., Warmack, R. J., Brown, G. M., Jacobson, K. B., Schrick, J, J. & Ferrell, T. L. (1992). Atomic force microscopy of DNA on mica and chemically modified mica. *Scanning Microsc.* **6**, 911–918.
Vesenka, J., Guthold, M., Tang, C. L., Keller, D., Delaine, E. & Bustamante, C. (1992). Substrate preparation for reliable imaging of DNA molecules with the scanning force microscope. *Ultramicroscopy,* **42–44**, 1243–1249.
Wyman, C., Grotkopp, E., Bustamante, C. & Nelson, H. C. M. (1995). Determination of heat-shock transcription factor 2 stoichiometry at looped DNA complexes using scanning force microscopy. *EMBO J.* **14**, 117–123.

Edited by D. E. Draper

(Received 30 July 1996; received in revised form 2 October 1996; accepted 2 October 1996)